

Washington Open File 175

UNITED STATES DEPARTMENT OF THE INTERIOR
GEOLOGICAL SURVEY

MASTER

Thermal surveillance of active volcanoes using the Landsat-1
data collection system.

PART III

Heat discharge from Mount St. Helens, Washington

by

Jules D. Friedman

U.S. Geological Survey, Denver, Colorado 80225

and

David Frank

U.S. Geological Survey, Seattle, Washington 98111

Open-File Report 77-541

1977

This report is preliminary and has not been edited or reviewed for conformity with U.S. Geological Survey standards and nomenclature

DISTRIBUTION OF THIS DOCUMENT IS UNLIMITED

14.25

Rev 8.3-78

274 7000

9508463

EW-78-X-05-1684

pey

DISCLAIMER

This report was prepared as an account of work sponsored by an agency of the United States Government. Neither the United States Government nor any agency Thereof, nor any of their employees, makes any warranty, express or implied, or assumes any legal liability or responsibility for the accuracy, completeness, or usefulness of any information, apparatus, product, or process disclosed, or represents that its use would not infringe privately owned rights. Reference herein to any specific commercial product, process, or service by trade name, trademark, manufacturer, or otherwise does not necessarily constitute or imply its endorsement, recommendation, or favoring by the United States Government or any agency thereof. The views and opinions of authors expressed herein do not necessarily state or reflect those of the United States Government or any agency thereof.

DISCLAIMER

Portions of this document may be illegible in electronic image products. Images are produced from the best available original document.

Heat discharge from Mount St. Helens, Washington

by

Jules D. Friedman

U.S. Geological Survey, Denver, Colorado 80225

and

David Frank

U.S. Geological Survey, Seattle, Washington 98111

Abstract

Two thermal anomalies, A at 2740 m altitude on the north slope, and B between 2650 and 2750 m altitude on the southwest slope at the contact of the dacite summit dome of Mount St. Helens, Washington, were confirmed by aerial infrared-scanner surveys between 1971 and 1973. Landsat-1 Data Collection Platform 6166, emplaced at site B anomaly, transmitted 482 sets of temperature values in 1973 and 1974, suitable for estimating the differential radiant exitance as 84 W m^{-2} , approximately equivalent to the Fourier conductive flux of 89 W m^{-2} in the upper 15 cm below the surface. The differential geothermal flux, including heat loss via evaporation and convection, was estimated at 376 W m^{-2} . Total energy yield of Mount St. Helens probably ranges between 0.1 and $0.4 \times 10^6 \text{ W}$.

Introduction

Mount St. Helens, Washington ($46^{\circ} 09' N$, $122^{\circ} 17' W$) was selected for Landsat-1 experiment SR 251, the thermal surveillance of active volcanoes, because of its history of eruptive activity in the 19th century and the possibility that it is an active, although presently quiescent, volcano (Fig. 1). Landsat-1 experiment SR 251 combined aerial infrared surveys with surface and near-surface temperature studies of volcanic thermal areas by means of the Landsat Data Collection System (DCS). Data Collection Platform (DCP) 6166 was located at about 3000 m elevation on the southwestern slope of Mount St. Helens, a few hundred meters below the summit, to investigate variations in surface temperatures and heat flux in a thermally anomalous area.

Statistical analysis of the temperature data obtained between July 1973 and April 1974 and derivative heat flux of the anomalous areas, as recorded by the aerial infrared surveys, are the main subjects of this report.

Acknowledgments

The authors thank Duane M. Preble and Tom Kollar of the Gulf Coast Hydrosience Center, USGS (U.S. Geol. Survey), for designing and constructing the Data Collection Platform and thermistor array instrument station, as well as Steve Hodge and Robert Krimmel for their assistance in emplacing the DCP installation on Mount St. Helens. The helicopter group of the 92d Aviation Company, U.S. Army, Paine Field, Everett, Washington, provided helicopter support

for installation of the DCP instrument station. George Van Tramp, Don Sawatzky and Gary Raines of the USGS designed new programs and applied existing computer programs for reduction and analysis of the DCP-derived temperature data, and Shirley Simpson assisted in data reduction.

The Mount St. Helens work was part of Landsat-1 experiment SR 251 carried out by the USGS under NASA Contract No. S70243AG, Task No. 434-641-14-03-04; permission for installation of DCP 6166 was granted by Burlington Northern, Inc. under Permit No. 7569. Aerial infrared scanner missions over Mount St. Helens were flown for the USGS by the U.S. Forest Service (USFS), Missoula, Montana, and Boise, Idaho, and by the Johnson Space Center, Houston, Texas.

Austin Post, USGS, provided oblique photographs of Mount St. Helens.

Geologic setting of Mount St. Helens

Mount St. Helens is a divergent stratovolcano formed of olivine basalt and pyroxene andesite flows through which several dacite domes have been erupted (Crandell and Mullineaux, 1973, p. A1). One of the dacite domes forms the present summit (Verhoogen, 1937; Hopson, 1971). The present volcano occupies the site of an ancestral dacitic volcanic center marked by remnants of five dacite domes and a thick lava lobe.

The late Holocene development of Mount St. Helens is divisible into 3 stages.

1. The early development of the present volcanic edifice of Mount St. Helens began with the growth of two dacite domes and eruption of andesitic lava flows, and culminated 500 years ago in aa flows of olivine basalt (Hopson, 1971, p. 138).
2. The summit-dome phase of development occurred about 450 years ago (Crandell, 1969) with the growth of a large dacite summit dome and subsequent flank eruptions of andesite flows.
3. The historic phase of activity occurred between 1802 and 1857 (Hopson, 1971, p. 138) and was marked by vulcanian eruptive activity with airfall pumice from a vent on the northwest flank, by growth of a dacite dome from this vent, and by flank eruptions of andesite from the northwest and south sides of the cone.

Surface thermal manifestations and infrared surveys

There are two known areas of fumaroles and warm ground on Mount St. Helens, (A) at "Boot Ridge" on the north flank at about 2740 m elevation, and (B) on the southwest flank at about 2740 m elevation. Both areas were reported by Lawrence (1939, p. 54). Later, Phillips (1941, p. 37-39) examined the (A) site on the north flank and found a cluster of fumaroles with maximum vapor temperature of 88°C.

Aerial infrared surveys were carried out for the present writers by the U.S. Forest Service and the National Aeronautics and Space Administration between April 1971 and April 1973; an earlier infrared

survey was made in 1966 (Moxham, 1970). Two of the infrared surveys, listed in Table 1, recorded thermal anomalies that correspond to both (A) and (B) areas of heat emission. These two surveys, conducted during the summers of 1966 and 1971 recorded the site (A) anomaly at 2740 m altitude along the east side of the Wishbone Glacier on the north slope of the mountain (Figs. 2 and 3). It seems likely that during the months of April and November when the other infrared surveys were made the (A) anomaly was not detected because of snow cover.

The larger thermal area at site (B) on the southwest slope was recorded in 1973 as a cluster of sharply defined anomalies, about 650 m^2 in area, between 2650 and 2750 m altitude. Anomalies at site (B) were also recorded in 1966 (Moxham, 1970), 1971, and 1972, but the first detailed ground reconnaissance of this area was made during the course of Landsat experiment SR 251. At present the anomalies at site (B) comprise five linear warm zones that extend down a talus slope. The warm ground is adjacent to two small remnants of stubby lava flows, near the contact between the summit dacite dome and the sliderock of the talus slope (Figs. 2, 4, 5, and 6). A dark red thermal alteration zone was observed along this contact. At the time of ground investigations of site (B) in 1972, no vapor emission was observed in this area, although a few small vents which have convected vapor at other times were found in the rubble. The above-mentioned observations of thermal activity on Mount St. Helens prior to the 1972 ground investigations reported here are summarized in Table 2.

Table 1.--Thermal Infrared Surveys of Mount St. Helens.

Date	Surveying Agency	Time	Time Zone	Scanner
9/4/66	USGS			
4/3/71	USFS, Boise	2040-2100	PDT	Recon XI
8/7/71	USFS, Boise	0448-0453	PDT	Recon XI
4/18/72	USFS, Missoula	2340-2355	PDT	RS-7
11/20/72	NASA, Houston	0416-0431	PST	RS-14
4/26/73	USFS, Missoula	0412-0459	PDT	RS-7

Table 2.--Summary of Recent Thermal Observations at Mount St. Helens.

<u>Date</u>		
<u>Area A, North flank, Boot Ridge, 2770 m</u>		
1939	Climber sighting	Hazard, 1932, referenced in Phillips, 1941, p. 37
7/13/41	Climber sighting Temperature - 61°C to 88°C	Phillips, 1941, p. 37-39
9/4/66	Thermal IR image, dim anomaly	Moxham, 1970, fig. 13
8/7/71	Thermal IR image, dim anomaly	USGS image by USFS, Boise

<u>Area B, Southwest flank, 2710 m</u>		
1939?	Climber sighting	Lawrence, 1939, p. 54, and Phillips, 1941, p. 37
5/6/65	Aerial photograph Bare rock, no steam	Photograph by Austin Post, USGS
4/3/71	Thermal IR image, bright anomaly	USGS image by USFS, Boise
4/18/72	Thermal IR image, dim anomaly	USGS image by USFS, Missoula
5/4/72	Aerial photograph Bare rock, no steam	Photograph by David Frank, USGS

Landsat-1 Data Collection Platform 6166

Landsat-1 Data Collection Platform 6166 was emplaced and operated at site (B) through the period July 20, 1973 to April 18, 1974, and was integrated with an 8-channel electronic thermal-sensor array whose characteristics are given in Table 3.

For a description of how the Landsat-1 Data Collection System functioned in experiment SR 251, see Friedman, Preble, and Jakobsson (1976, p. 653-657), and Friedman, Frank, Preble, and Jakobsson, (1976, p. 36-47). For details of the electronic thermal-sensing systems designed, constructed and operated in experiment SR 251, see Preble, Friedman, and Frank (1976, p. 1-64) who also give details of the DCP's and electronic integration of the thermal-sensing systems and the DCP's.

Statistical analysis of DCP temperature data from site B

Correlation analysis of temperature variations (Table 4) recorded by DCP 6166, emplaced at site (B), Mount St. Helens, Washington, was carried out by derivation of correlation coefficients to indicate the degree of probability of a linear relationship between each of the data sets. The correlation coefficients and their statistical significance are given in Tables 5 and 6.

The following interpretation emerges from the correlations. The instrument-station temperatures were influenced by both air and warm ground (on which the installation was located). Cool ground temperature variations show a 56.8% correlation with air temperature

Table 3.—Data Collection Platform 6166, Mount St. Helens, Washington, July 20, 1973–April 18, 1974.
46°9'N, 122°17'W; elevation = 2700 m MSL.

DCP analog channel	Sensor type and number	Probe site and depth	Sensor temperature range and accuracy (°C)	Relationship between output voltage and temperature (T°C)
1	YSI 44203	Instrument station (inside enclosure)	-40 to 60 \pm 2	T = -40 + 20 (V)
2	YSI 44203	Ambient air 1 m above ground (protected from sun)	-40 to 60 \pm 2	T = -40 + 20 (V)
3	YSI 44203	Cool ground surface	-10 to 40 \pm 1	T = -10 + 10 (V)
4	YSI 44201	Resistor plug	N.A.	N.A.
5	YSI 44201	15-cm depth in warm ground	5 to 75 \pm 1	T = 5 + 14 (V)
6	YSI 44201	Warm ground surface	5 to 75 \pm 1	T = 5 + 14 (V)
7	YSI 44201	15-cm depth in warm ground	5 to 75 \pm 1	T = 5 + 14 (V)
8	104MB	50-cm depth in warm ground	0 to 100 \pm 1	T = 20 (V)

Table 4.--Statistical Analysis of Temperature Data, Mount St. Helens, Washington, July 1973 to April 1974.

DCP Analog Channel	Probe site and depth	Mean temp.	Standard deviation	Min. Temp.	Max. Temp.	Variance	Skewness	Kurtosis	Coefficient of variation (C)	
		($^{\circ}$ W $^{\circ}$ C)	(S)	($^{\circ}$ C)	($^{\circ}$ C)	(S ²)			Based on Celsius	Based on Kelvin
1	Instrument station (inside enclosure)	29.4	± 15.0	3.1	60.0	225.2	0.4	-0.6	.51	.05
2	Ambient air 1-m above ground (protected from sun)	12.9	± 8.5	- 5.1	49.0	72.8	0.5	0.6	.66	.03
3	Cool ground surface	13.5	± 5.7	2.6	35.0	32.9	0.6	-0.1	.42	.02
5	15-cm depth in warm ground	49.1	± 4.7	2.6	65.9	22.4	-2.2	21.7	.10	.01
6	Warm ground surface	28.4	± 5.2	9.1	49.5	36.7	0.2	1.9	.18	.02
7	15-cm depth in warm ground	39.6	± 5.6	19.0	58.8	31.5	0.5	1.6	.14	.02
8	50-cm depth in warm ground	60.8	± 8.3	42.3	89.0	69.2	1.2	0.1	.14	.02

Table 5.--Correlation Coefficients (r) Between Temperature Data
Recorded by DCP 6166 Between July 20, 1973 and April 18,
1974, Mount St. Helens, Washington.

DCP Channel	1	2	3	5	6	7	8
1	1.000	0.585	0.626	0.217	0.410	0.332	0.274
2	0.585	1.000	0.568	0.284	0.420	0.406	0.572
3	0.626	0.567	1.000	0.244	0.515	0.251	0.023
5	0.217	0.284	0.244	1.000	0.168	0.310	0.283
6	0.410	0.420	0.515	0.168	1.000	0.849	0.377
7	0.332	0.406	0.251	0.310	0.849	1.000	0.668
8	0.274	0.572	0.023	0.283	0.377	0.668	1.000

Table 6.--Significance of statistical correlation of selected temperature variations, Mount St. Helens, Washington, between July 20, 1973, and April 18, 1974. 482 data transmission.

DCP channels correlated		Linear correlation coefficient(r)	Confidence	Significance (probability that a linear relationship exists)
1 vs. 2	Instrument station vs. ambient air 1-m above ground	0.585	>99.9	Very highly significant
3 vs. 2	Cool ground vs. ambient air	0.568	>99.9	Very highly significant
3 vs. 6				
5 vs. 7	Two 15-cm depth probes at different locations	0.310	99.0	Highly significant
5 vs. 2	15-cm depth vs. ambient air	0.284	99.0	Highly significant
5 vs. 8	15-cm depth vs. 50-cm depth in warm ground	0.283	99.0	Highly significant
5 vs. 3	15-cm depth vs. cool ground surface	0.248	98.0	Significant
6 vs. 7	Warm ground surface vs. 15-cm depth in warm ground	0.849	>99.9	Very highly significant
6 vs. 3	Warm ground surface vs. cool ground surface	0.515	>99.9	Very highly significant
6 vs. 2	Warm ground surface vs. ambient air	0.420	>99.9	Very highly significant
6 vs. 8	Warm ground surface vs. 50-cm depth in warm ground	0.377	>99.9	Very highly significant

Table 6.--(continued)

7 vs. 6	15-cm depth vs. 50-cm depth in warm ground	0.849	>99.9	Very highly significant
7 vs. 8	15-cm depth vs. ambient air	0.406	>99.9	Very highly significant
7 vs. 2	15-cm depth vs. ambient air	0.406	>99.9	Very highly significant
7 vs. 5	15-cm depth vs. ambient air	0.310	99.0	Highly significant
8 vs. 7	50-cm depth (warm) vs. 15-cm depth (warm ground)	0.668	>99.9	Very highly significant
8 vs. 2	50-cm depth vs. ambient air	0.572	>99.9	Very highly significant
8 vs. 6	50-cm depth vs. warm ground surface	0.377	>99.9	Very highly significant
8 vs. 5	50-cm depth vs. 15-cm depth (warm)	0.283	92.0	Highly significant
8 vs. 3	50-cm depth vs. cool surface	0.022	None	Not significant

and a 51.5% correlation with warm ground temperatures, suggesting that the cool ground has some similarities in temperature characteristics to the warmer ground and might be marginally geothermal. Hence the mean ground temperatures from Probe 3 (DCP Analog channel 3) are probably slightly higher than the cold-base reference temperature for the area. Since the mean ambient air temperature is only 0.6°C cooler than the mean temperature of Probe 3, the geothermal influence at Probe 3 may be on the order of or less than 3 W m^{-2} or 75 HFU.

The temperature variations from the two 15-cm depth probes in warm ground show a significant mutual correlation but a somewhat different relation with other data sets. Both 15-cm probes show the influence of geothermally warm ground at greater depths and of ambient-air temperatures, but while these influences are almost equally balanced at Probe 5, temperatures from Probe 7 show a closer relationship to deeper geothermal temperatures. The warm ground-surface temperatures show the influence of both geothermal temperatures at shallow depth and of ambient-air temperatures. Similarly, temperatures at 50-cm depth in warm ground show a close relation to 15-cm depth, warm-ground surface, and ambient air-temperature variations, but no significant relation to cool surface temperatures.

Heat flux of site B anomaly, southwest flank of Mount St. Helens

Assumption: below the surface, conduction is the dominant mode of transfer while heat exchange from the surface to the atmosphere is by radiation

Fourier conductive flux in the upper 50 cm below the surface.

The heat flux at site B may be estimated by the following equation for the Fourier conductive flux q

$$q = \frac{kA}{L} (t_1 - t_2) ,$$

where k is the thermal conductivity in calories per square centimeter per second, A is the area in square centimeters, L is the length of section measured in centimeters, t_1 is the mean 50-cm temperature recorded by DCP 6166 (Table 4) from the thermal-sensor array; t_2 is the mean surface temperature of the anomaly. The thermal conductivity, k , of the andesite-dacite surface is estimated at $0.002 \text{ cal cm}^{-1} \text{ s}^{-1}$, typical of similar materials reported in the literature.

The Fourier heat flux, q , between the surface and a depth of 50 cm at site B, DCP 6166, is $1300 \mu \text{ cal cm}^{-2} \text{ s}^{-1}$ or 54 W m^{-2} . Between the surface and 15-cm depth, q equals $2100 \mu \text{ cal cm}^{-2} \text{ s}^{-1}$ or 89 W m^{-2} .

Differential radiant exitance from the surface. The differential radiant flux or exitance is a measure of the heat exchange with the atmosphere as the result of conductive warming of the earth's surface. The differential radiant exitance from one point in relation to a second point that radiates heat to a common atmosphere can be estimated by application of a two-point thermal model (Friedman and Frank, 1977, p. 16-17). Specifically, the differential radiant exitance, $Wd\lambda$ (the differential power radiated per unit area for

the earth's surface) is derived from the Stefan-Boltzmann function via the following expression,

$$Wd\lambda = \epsilon 5.679 \times 10^{-12} (T_1^4 - T_2^4) ,$$

where emissivity ϵ is $0.98_{\pm 0.02}$, T_1 is the mean temperature (301.5°K) of a warm surface (Table 4, Probe 6), and T_2 is 286°K (Table 4, Probe 3), the mean temperature of a cold standard-reference surface.

The differential radiant exitance by this method is $2000 \mu \text{ cal cm}^{-2} \text{ s}^{-1}$ or 84 W m^{-2} .

Assumption: evaporation, convection, and conduction are important in heat exchange with the atmosphere

Differential geothermal flux based on heat balance of ground surface. The two-point model for heat balance of the ground surface (Sekioka and Yuhara, 1974) for estimating volcanogenic heat flows considers the following factors: the net outgoing radiant flux, the nocturnal radiation, heat flow in the ground due to solar radiation, heat flow to the atmosphere via eddy diffusion, evaporative heat exchange with the atmosphere, and the geothermal (i.e., volcanogenic) flux. The two-point model permits the following simplified relationship (Sekioka and Yuhara, 1974, p. 2056)

$$\Delta G = \epsilon(1 - 0.09M) 0.52 + 0.065 (e_w)^{\frac{1}{2}} \sigma \Delta(T_o^4) \\ + p_a c_p D(1 + \lambda) \Delta\theta ,$$

in which the differential geothermal flux ΔG is expressed in terms of effective surface emissivity ϵ ($0.98_{\pm 0.02}$), cloudiness M (6.16,

average during the period July 1973 to April 1974), vapor pressure e_w (4.1 m bar), the Stefan Boltzmann constant σ , surface temperature of anomalous area T_o (301.5°K, Table 4, Probe 6) and θ (28.4°C), air density p_a (0.909×10^{-3} g cm⁻³ at 3000 msl), the coefficient of diffusion of water vapor into air D (1.59 cm s⁻¹) and the Bowen ratio R (0.3, the ratio of heat lost from the surface by eddy diffusion and conduction to heat lost by evaporation at 0 wind speed, Friedman and Frank, 1977, p. 36).

The differential geothermal flux, at DCP 6166, site B, by the above model is 9000 μ cal cm⁻² s⁻¹ or 376 W m⁻².

Total heat discharge from site B anomaly

If the heat flux of 376 W m⁻² is uniform throughout the site B anomaly, the total heat discharge would be 0.24×10^6 W. This should be regarded as a maximum heat loss. Using the conductive heat flux or differential radiant exitance as a base, the total discharge would be 0.06×10^6 W, a minimum value.

Total heat discharge from Mount St. Helens thermal anomalies

The site A anomaly is smaller than that at site B. Considering both site A and B anomalies, and the range between minimum and maximum heat flux, the total heat discharge from Mount St. Helens ranges between 0.1 and 0.4×10^6 W.

Summary and conclusions

Five aerial infrared line-scan surveys between April 1971 and April 1973 confirmed the existence and delimited the boundaries of two thermal anomalies on the surface of the upper slopes of Mount St. Helens. Site A anomaly is at 2740 m altitude along the east side of the Wishbone Glacier on the north slope, site B anomaly forms a cluster of five sharply defined linear zones about 650 m² in area between 2650 and 2750 m altitude on the southwest slope, near the contact of the summit dacite dome.

Data Collection Platform 6166 emplaced at the site B anomaly, transmitted temperatures from the instrument station, ambient air, thermal and non-thermal ground surfaces, and from probes at 15- and 50-cm depths. Statistical analysis of 482 data transmissions via Landsat-1 between July 1973 and April 1974, provided the basis for estimating the differential radiant exitance at site B at about 84 W m⁻² or 2000 μ cal cm⁻² s⁻¹, equivalent to the Fourier conductive flux in the upper 15 cm below the ground surface. The Fourier conductive flux between the surface and 50-cm depth was 54 W m⁻² or 1300 μ cal cm⁻² s⁻¹. The differential geothermal flux at site B, based on the heat balance of the ground surface, and considering evaporation, diffusion, conduction, and radiation contributions to heat exchange with the atmosphere, is considerably greater, about 376 W m⁻² or 9000 μ cal cm⁻² s⁻¹.

Total heat discharge from Mount St. Helens is estimated at between 0.1 and 0.4 x 10⁶ W.

Abbreviations and symbols

A	=	area in cm^2
C	=	coefficient of variation
D	=	coefficient of diffusion of water vapor into the atmosphere
DCP	=	Data Collection Platform (Landsat-1)
DCS	=	Data Collection System (Landsat-1)
ΔG	=	differential geothermal flux
e^w	=	vapor pressure
ϵ	=	effective surface emissivity
HFU	=	Heat Flow Unit, equivalent to one microcalorie per centimeter squared, or .04 watt per meter squared
IR	=	infrared
k	=	thermal conductivity, in calories per centimeter per second
L	=	length of section measured for Fourier conductive heat flow estimate
M	=	cloudiness, on a scale of 10
ω	=	sample mean
$\mu \text{ cal}$	=	microcalorie (10^{-6} cal)
p_a	=	air density
q	=	Fourier conductive flux
R	=	Bowen ratio
r	=	linear correlation coefficient
S	=	mean standard deviation
S^2	=	variance

σ = Stefan-Boltzmann constant (see Glossary for Stefan-Boltzmann Function)
 T_o = mean surface temperature ($^{\circ}\text{K}$) of anomalous area in differential geothermal flux equation
 T_1 = mean temperature ($^{\circ}\text{K}$) of geothermal surface
 T_2 = mean temperature ($^{\circ}\text{K}$) of cold reference surface in differential radiant exitance equation
 t_1 = mean 50-cm depth temperature in Fourier conduction equation
 t_2 = mean surface temperature in Fourier conduction equation
 θ = mean surface temperature ($^{\circ}\text{C}$) of anomalous area in differential geothermal flux equation
 USFS = United States Forest Service
 USGS = United States Geological Survey
 V = volts
 W = watts
 $Wd\lambda$ = differential radiant power radiated per unit area from the earth's surface
 YSI = Yellow Springs Instrument Corporation (thermistor probe)

References cited

- Crandell, D. R., 1969, The geologic story of Mt. Rainier: U.S. Geol. Survey Bull. 1292, 43 p.
- Crandell, D. R., and Mullineaux, D. R., 1973, Pine Creek volcanic assemblage at Mount St. Helens, Washington: U.S. Geol. Survey Bull. 1383-A, 23 p.
- Friedman, J. D., Frank, David, Preble, D. M., Jakobsson, Sveinn, 1976, Thermal surveillance of active volcanoes using the Landsat-1 Data Collection System. Preface and Part 1: The Surtsey, Iceland temperature data relay experiment via Landsat-1: Final report for experiment SR-251: U.S. Geol. Survey for Goddard Space Flight Center, 55 p. Available through Nat. Tech. Inf. Service, Springfield, Va.
- Friedman, J. D., Preble, D. M., and Jakobsson, Sveinn, 1976, Geothermal flux through palagonitized tephra, Surtsey, Iceland--The Surtsey Temperature-data-relay experiment via Landsat-1: Jour. Research, U.S. Geol. Survey, v. 4, no. 6, p. 645-659.
- Friedman, J. D., and Frank, David, 1977, Infrared surveys, radiant flux and total heat discharge from Mount Baker volcano, Washington, between 1970 and 1975: Thermal surveillance of active volcanoes using the Landsat-1 DCS. Part 2. Final report: U.S. Geol. Survey for Goddard Space Flight Center, 63 p. Available through Nat. Tech. Inf. Service, Springfield, Va.
- Hopson, C. A., 1971, Eruptive sequence at Mount St. Helens, Washington: Geol. Soc. America, Cordilleran Sec., Abs. with Programs, v. 3, no. 2, p. 138.

- Lawrence, D. B., 1939, Continuing research on the flora of Mount St. Helens: *Mazama*, v. 21, no. 12, p. 49-54.
- Moxham, R. M., 1970, Thermal features at volcanoes in the Cascade Range, as observed by aerial infrared surveys: *Bull. Volc.*, v. 34, no. 1, p. 77-106.
- Phillips, K. N., 1941, Fumaroles of Mount St. Helens and Mount Adams: *Mazama*, v. 23, no. 12; p. 37-42.
- Preble, D. M., Friedman, J. D., and Frank, David, 1976, Thermal surveillance of active volcanoes using the Landsat-1 Data Collection System. Part 5: Electronic thermal sensor and Data Collection Platform technology: U.S. Geol. Survey for Goddard Space Flight Center, 64 p. Available through Nat. Tech. Inf. Service, Springfield, Va.
- Sekioka, Mitsuru, and Yuhara, Kozo, 1974, Heat flux estimation in geothermal areas based on the heat balance of the ground surface: *Jour. Geophys. Res.*, v. 79, no. 14, p. 2053-2058.
- Verhoogen, Jean, 1937, Mount St. Helens--a recent Cascade volcano: *California Univ. Pub. Geol. Sci.*, v. 24, no. 9, p. 263-302.

Illustrations

Figure 1.--Index map of the Mount St. Helens region. Modified from Crandell and Mullineaux, 1973.

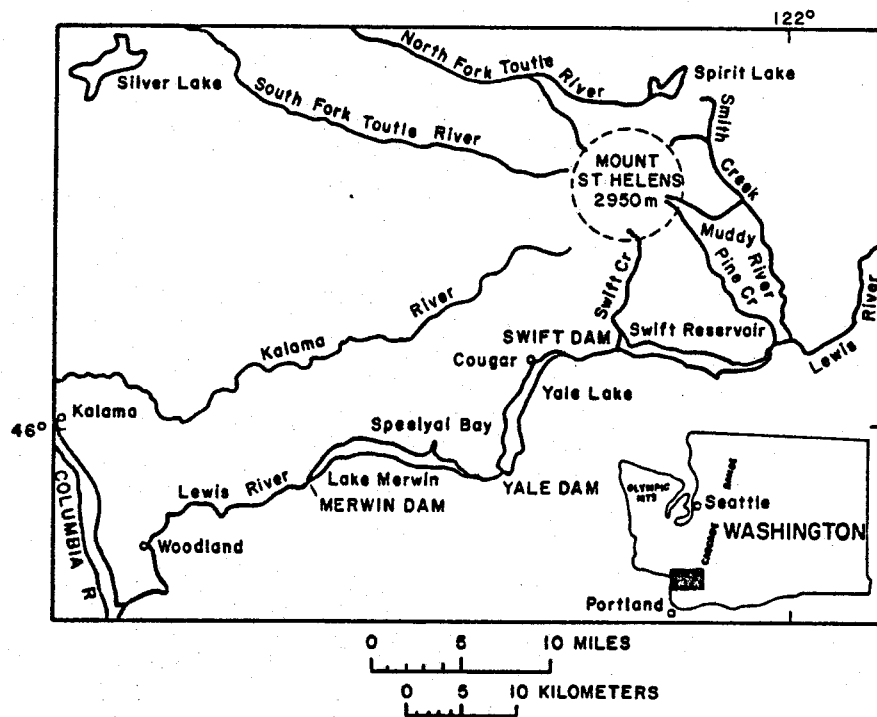
Figure 2.--Infrared anomalies A and B, shown in solid black, near the summit of Mount St. Helens. Anomalies correspond to area of warm ground and weak fumarolic activity. Landsat-1 Data Collection Platform 6166 and electronic thermal sensing system were located at site B between 1973 and 1976. Boundaries of permanent snow and ice fields are represented by dashed lines. Anomalous areas were mapped by aerial infrared scanner between 1970 and 1973. Summit of Mount St. Helens is at approximately $46^{\circ} 12' \text{ N}$ and $122^{\circ} 15' \text{ W}$.

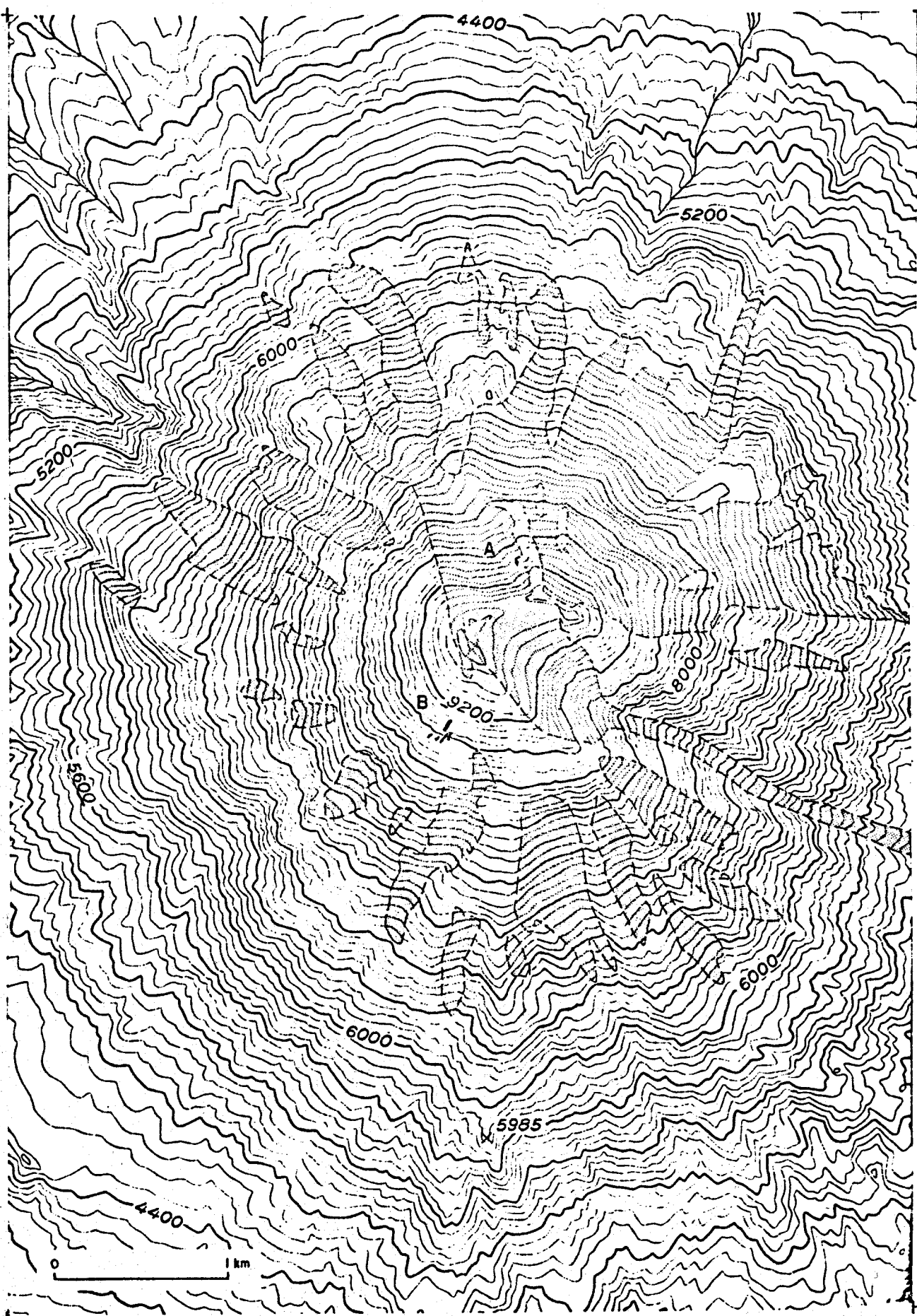
Figure 3.--Northwest slope of Mount St. Helens showing the area of site A thermal anomalies and weak fumarolic activity at "The Boot" above Wishbone Glacier. Photograph R2-62-73-1 September 7, 1962, by Austin Post.

Figure 4.--Southwest slope of Mount St. Helens showing the area of site B thermal anomalies at the contact between the summit dacite dome and the extensive talus slopes. Data Collection Platform 6166 was installed at this location. Photograph R2-62-74, September 1962 by Austin Post.

Figure 5.--Site B thermal anomalies on southwest slope of Mount St. Helens near the summit. Note dark area where snow cover has melted over warm ground. May 4, 1972.

Figure 6.--Closeup of thermal area of site B showing detail of snow-melt pattern over linear zones. May 4, 1972.







Wishbone

SEPT 7 - R 62-7





